COMMUNICATION

Microwave-assisted functionalization of carbon nanohorns with oligothiophenes units with SERS activity

Received 00th January 20xx,
Accepted 00th January 20xx

DOI: 10.1039/x0xx00000x

Daniel Iglesias,[a] Javier Guerra,[b] María Isabel Lucío,[c] Rafael C. González-Cano,[d] Juan T. López Navarrete, [d] M. Carmen Ruiz Delgado, [d] Ester Vázquez, [e,f] M. Antonia Herrero*[e,f]

Carbon nanohorns have been functionalized with oligothiophene units *via* the 1,3-dipolar cycloaddition reaction under microwave irradiation and solvent-free conditions. A dramatic Raman enhancement was found for one of the synthesized derivatives. Experimental and *in silico* studies helped to understand the enhancement, attributed to the modification of electromagnetic fields upon the functionalization at the tip of the nanostructures.

Nanotechnology burst with the fast improvement of characterization techniques and the development of new nanomaterials. This multidisciplinary field is called to overcome many of the most important challenges that the scientific community is facing nowadays, such as the development of fast and reliable imaging. In this regard, surface-enhanced Raman spectroscopy (SERS) is a very powerful technique.[1] The absence of autofluorescence, the narrow spectral lines and the possibility to obtain multiple colors with a single excitation wavelength in a region with low background make Raman imaging an ideal candidate in bio-imaging.[2] For instance, the G-mode of isotopically modified single-walled carbon nanotubes (CNTs) was engineered and displayed three different colors in Raman imaging.[3] Two different effects, often called field enhancement (FE) and chemical enhancement (CE), are the responsible for the magnification observed in SERS. FE, attributed to the interaction between an appropriate wavelength and metal particles or surfaces, yields greater enhancements than CE. CE results from the interaction between the material surface and the adsorbed molecule, usually involving electronic effects such as charge-transfer processes.[4] This factor depends on the electronic interaction between the adsorbate and the substrate, which requires a specific match in a singular chemical site on the surface. CE is limited to very short distances. Additionally, resonance Raman enhancement is observed when the excitation wavelength falls within an electronic transition of the molecule (*e.g.* HOMO-LUMO).[5]
The finest material engineering techniques have allowed the development of very powerful SERS substrates. For instance, Bodegón et *al.* embedded plasmonic structures (*i.e.* Au nanorods, nanospheres or nanorods plasmonic crystals) in various matrices (*i.e.* a polymeric hydrogel, mesoporous TiO_2, or mesoporous SiO_2, respectively) to track pyocyanin down to 10^{-14} M, which allowed them to follow the *quorum sensing* in bacteria films.[6] Nanomaterials synthesis and functionalization determines their performance. For instance, the so-called graphene-enhanced Raman scattering requires the precise synthesis of monolayer graphene. Otherwise, the enhancement decreases as the number of layers increases.[5] In another example, the Fermi energy (E_f) of CVD graphene was tuned by introducing N atoms in the 2D lattice during the synthesis.[7] The modified E_f was closer to the LUMO orbitals of the analytes than the E_f of pristine graphene (*i.e.* without N atoms), which makes it easier the charge-transfer process responsible for the Raman enhancement, sensing rhodamine B down to 10^{-11} M. The latter and other works show the potential of carbon nanomaterials in this field,[4,8,9] where only few of them reported SERS effect in the absence of metals. Surprisingly, the potential of carbon nanohorns (CNHs)[10] has been scarcely investigated until now.

Further development of nanomaterials for Raman imaging and sensing will require a deep understanding of the systems. Recently, we reported, to the best of our knowledge, the first example of Raman enhancement using CNHs.[11] A series of di-, tri- and tetra-substituted oligothiophenephenylvinylene dendrons were non-covalently attached to CNHs. The substitution pattern of the molecules strongly influenced the

[a] *Université de Strasbourg, CNRS, ISIS, 8 allée Gaspard Monge, 67000 Strasbourg, France*
[b] *Facultad de Ciencias, Universidad de Valladolid, 47011, Valladolid, Spain*
[c] *Instituto Interuniversitario de Investigación de Reconocimiento Molecular y Desarrollo Tecnológico (IDM), Universitat Politècnica de València, Universitat de València, Camino de Vera s/n, 46022 Valencia, Spain.*
[d] *Department of Physical Chemistry, University of Malaga, Campus de Teatinos s/n, Malaga 29071, Spain.*
[e] *Facultad de Ciencias y Tecnologías Químicas, Universidad de Castilla-La Mancha (UCLM), 13071 Ciudad Real, Spain. E-mail : MariaAntonia.Herrero@uclm.es*
[f] *Instituto Regional de Investigacion Científica Aplicada (IRICA), 13071 Ciudad Real, Spain*
Electronic Supplementary Information (ESI) available: [details of any supplementary information available should be included here]. See

molecule-CNH interaction. Thus, tri-substituted dendrons interacted via π-π stacking, while CH-π interaction was prevailing for the di- and tetra- analogues, which appeared to be bended around the CNH to maximize the interaction. Interestingly, the latter developed significantly higher Raman enhancement.

The possibility to develop SERS activity with nanomaterials of wide-ranging chemical nature is clear. In turn, nanomaterial morphology is also a key factor. The subject has been largely explored for metal nano-assemblies,[12,13] yet scarcely investigated for the differently shaped carbon nanomaterials. In this work, we have carried out a fast, eco-friendly and scalable methodology to synthesize functionalized CNHs (*f*-CNHs) with thiophene units in a controlled manner. Three different derivatives have been used to evaluate the influence of functionalized CNHs when increasing the number of thiophene units. The characterization of the materials unequivocally showed the covalent functionalization and revealed a significant Raman enhancement on certain derivatives, which makes them suitable candidates in the field of multi-color Raman imaging. Density functional theory (DFT) calculations were performed to study this phenomenon *in silico*. Besides, functionalized CNTs (*f*-CNTs) and non-covalently functionalized CNHs were prepared to assess the effect of carbon nanostructure morphology and the nature of the interaction between the molecules and the CNHs.

Functionalization of CNHs was achieved via 1,3-dipolar cycloaddition (Fig. 1 top). The reaction involves generation of azomethine ylides *in situ* upon the thermal condensation of an α-amino acid and an aldehyde.[14,15] In this case, glycine and three different aldehydes with increasing number of thiophene units (*i.e.* one, two or three units for aldehyde 1, 2 or 3, respectively) and CNHs were reacted under microwave irradiation and solvent-free conditions following experimental conditions previously reported in our group.[15] The method provided functionalized CNHs with *N*-pyrrolidines substituted with the corresponding thienyl unit. The five-membered heterocycles are integrated covalently in the nanostructures. This increases their stability in contrast to non-covalently *f*-CNHs, which rely on weaker supramolecular interactions (*e.g.* π-π stacking). In addition, the reproducibility of the applied synthetic method is superior to most non-covalent approaches. Both stability and reproducibility are important aspects that must be accomplished for the global implementation of SERS applications.[1] As main drawback, covalent functionalization comes at the expenses of the graphitic structure. Transmission electron microscopy confirmed that the unique structure of CNHs was not compromised (Fig. 1a, see Fig. S1 ESI† for the morphological characterization of *p*-CNH). The functionalization was established by thermogravimetric analysis (TGA) (Fig. 1b), which permitted to quantify the degree of functionalization by comparing the thermal stability of *p*-CNH and *f*-CNHs at 550 °C. The calculated values were 866, 574 and 448 μmol/g for *f*-CNH 1, *f*-CNH 2 and *f*-CNH 3, respectively. The increase of defectiveness in functionalized CNHs was assessed by Raman spectroscopy (Fig. 1c). Pristine CNHs (*p*-CNH) display the graphitic peak (G-band, ~1595 cm^{-1}) and a high-intensity defect related mode (D-band, ~1320 cm^{-1}) due to the curved structure and the presence of amorphous carbon inside the cluster.[16] The relative intensity between the D- and G-bands (*i.e.* I_D/I_G ratio, 1.04 for *p*-CNH) increased in all cases being 1.32 for *f*-CNH 1 (one thiophene unit), 1.42 for *f*-CNH 2 (two thiophene units) and 1.16 for *f*-CNH 3 (three thiophene units). According to the Raman spectra and TGA, the degree of functionalization decreased when the number of thiophene units increased. This effect is likely due to the steric hindrance and the different melting points of the aldehydes (*i.e.* liquid at room temperature, 55-58 °C, and 141 °C for aldehydes 1, 2 and 3, respectively), which is markedly important in solvent-free conditions.

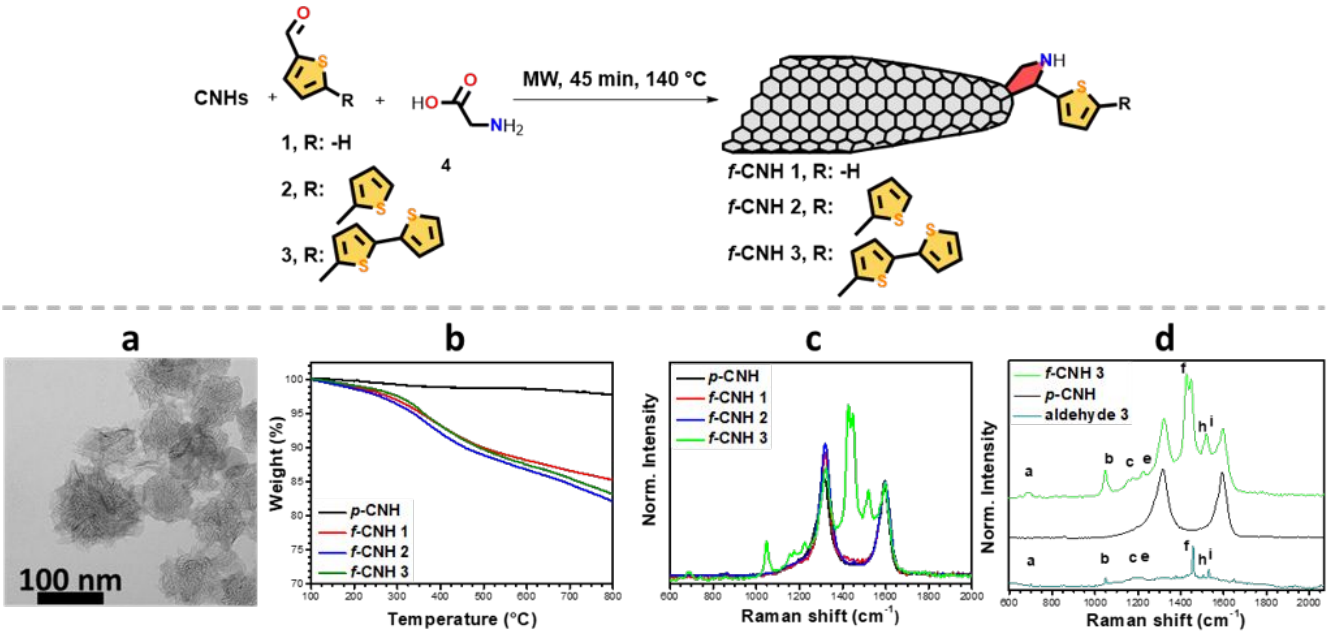

Fig. 1.(Top) Synthesis of *f*-CNHs. (Bottom) Characterization of *f*-CNHs showing (a) TEM of *f*-CNH 3, (b) TGA and (c) Raman spectra of all derivatives; and (d) comparison of the Raman spectra with the spectrum of aldehyde 3. Letters in picture d are linked to signals that are denoted along the text. Similar results were obtained when sarcosine was the used amino acid (Fig. S2 ESI†)

Outstandingly, the Raman spectrum of *f*-CNH 3 displayed the bands related to *p*-CNH and some unexpected additional bands. Most of these bands were attributed to the grafted terthienyl moiety by comparison with the Raman spectrum of aldehyde 3, which revealed a significant Raman enhancement (Fig. 1d). The sharp and high intensity band at 1427 cm^{-1}, denoted as **f**, could be useful in CNHs-based multi-color Raman imaging. To gain insight into the enhancement phenomenon, several experimental and *in silico* investigations were performed.

Firstly, *p*-CNH were non covalently functionalized with aldehyde 3 (control-CNH) to evaluate the importance of the nature of the interaction (*i.e.* covalent vs supramolecular) (Fig. S3, ESI†). Control-CNH were prepared following a protocol reported by some of us.[11] The Raman spectrum of control-CNH showed a negligible trace of aldehyde 3. The low Raman signal of the supramolecular derivative (control-CNH) in comparison with *f*-CNH 3 ruled out that the enhanced Raman modes are due to the adsorbed aldehyde molecules. Secondly, CNTs, chosen as unidimensional analogue of CNHs, were covalently functionalized using glycine and aldehyde 3 (*f*-CNT 3) to assess the effect of carbon nanostructure morphology. TGA and Raman spectroscopy confirmed the functionalization, however the enhancement of Raman bands was not observed (Fig. S4, ESI†).

DFT calculations were implemented to understand the molecular and electronic structure of the functionalized nanomaterials. In agreement with previous DFT studies,[17] larger binding energies were obtained for the sites close to the cone tip when compared to the lateral configurations (Fig. S5 ESI†). Therefore, the tip configuration was chosen as reference for the remaining work.

The theoretical Raman spectrum of aldehyde 3 nicely predicted the most intense bands experimentally observed and helped to their assignments (Fig. 2). The band at 1457 cm^{-1} (denoted as **f**) is ascribed to an in-phase C_α=C_β stretching vibration delocalized along the whole π-conjugated oligothiophene backbone calculated at 1442 cm^{-1} and the bands at 1506 and 1531 cm^{-1} (denoted as **h** and **i**, and calculated at 1495 and 1518 cm^{-1}, respectively) are attributed to an out-of-phase C_α=C_β stretching vibration localized in the internal and external thiophene units, respectively (see their corresponding eigenvectors in Fig. S6, ESI†). Importantly, when analysing the theoretical Raman spectrum of *f*-CNH 3, besides the bands associated to the D and G modes, a very intense band predicted at 1456 cm^{-1} (band **f**) emerged, which is ascribed to the collective C_α=C_β stretching vibration of the terthienyl unit (see the eigenvector in Fig. 2b). It is interesting to note that the Raman activity of the band **f** is even larger than that associated with the G band in *f*-CNH 3, and also six times larger when compared with the homologue C_α=C_β stretching vibration calculated in aldehyde 3. However, in contrast to the enhancement observed in CNHs, no selective Raman intensification was observed in the analogues *f*-CNT 3 (Fig. 2a).

Our calculations showed that the relative orientation of the terthienyl unit with respect to the cone tip is crucial for the

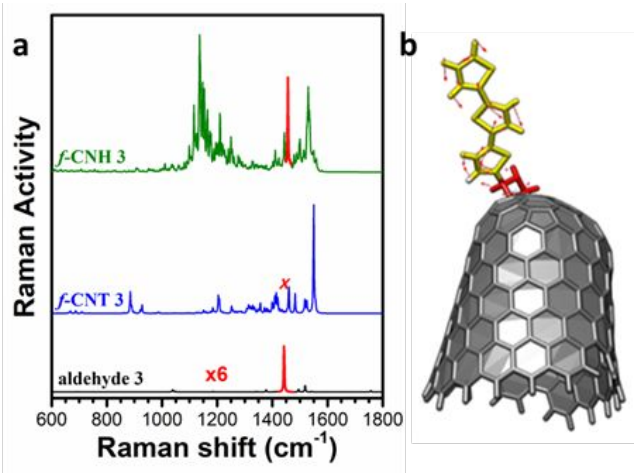

Fig. 2. (a) Theoretical Raman spectra of aldehyde 3, *f*-CNT 3 and *f*-CNH 3. Note that spectrum of aldehyde 3 has been amplified by a factor of 6. (b) The eigenvector associated with the normal mode calculated at 1456 cm^{-1} (band **f**, highlighted with a red line in the spectrum) for *f*-CNH 3. A comprehensive table with the experimental and calculated bands (Table S1, ESI†) and the experimental enhancement (Fig. S7, ESI†) for *f*-CNH 3 are reported in the supporting information.

selective enhancement of the Raman bands. For instance, the largest Raman activity of the collective C_α=C_β stretching modes of the terthienyl unit was observed for the configuration where the grafted molecule is largely bent towards the cone tip (49°) (denoted as tip 2 configuration in Fig. S3 and Fig. S8, ESI†). As seen in Fig. 3a and 3b, a HOMO-LUMO gap decrease of 0.30 eV was found in *f*-CNH 3 with tip configurations as compared to the non-functionalized *p*-CNH; this was associated to a HOMO destabilization and a LUMO stabilization upon functionalization on the conical tip. Note that the HOMO displayed a larger electron density around the lateral surface of the CNH and the LUMO was mostly located on the pentagons of the conical tip linked to the pyrrolidine unit, thus, suggesting a certain amount of charge-transfer towards the conical tip of *f*-CNH 3. This is in good accordance with the Mulliken atomic charge distribution that indicated that the terthienyl units are positively charged, while the CNHs are negatively charged (Fig. 3c). The change in the C-C bond length alternation (BLA) pattern of the pyrrolidine units from positive to negative values when the units are attached to CNHs is a consequence of the intramolecular charge-transfer from the oligothienyl spine towards the CNHs conical tip (see Table S2, ESI†). In contrast, the HOMO-LUMO gap and the HOMO and LUMO wavefunctions of CNTs are slightly affected upon functionalization (Fig. 3); this is in agreement with the calculated atomic charge distribution and BLA values (Table S3, ESI†) that indicates an absence of charge-transfer character in this particular case from the oligothienyl backbone towards CNTs.

Interestingly, the amount of charge-transfer towards the conical tip was considerably less pronounced for CNHs functionalized with one or two thiophene units (Fig. S9 and S10, ESI†). This effect results in a decrease of the selective enhancement of the Raman scattering of the collective C=C stretching modes associated to the oligothiophene backbone

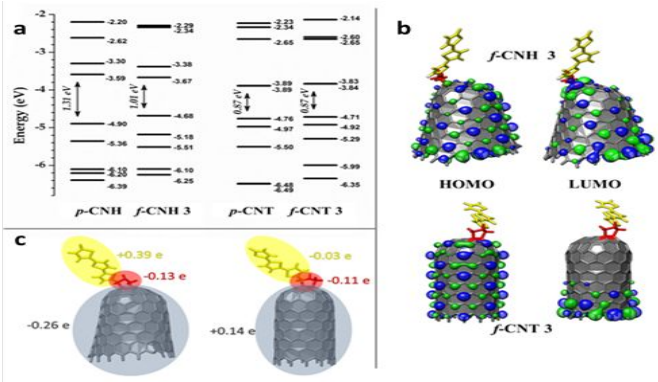

Fig 3. (a) DFT-calculated molecular orbital energies (M06-2X/6-31G** level) for *p*-CNHs, *f*-CNH 3, *p*-CNT and *f*-CNT 3. (b) Topologies of the frontier molecular orbitals and (c) Mulliken atomic charges on different molecular domains for *f*-CNH 3 and *f*-CNT 3.

when comparing *f*-CNH 1 and *f*-CNH 2 with *f*-CNH 3 (Fig. S11, ESI†).

Thus, the spectral Raman enhancement observed in functionalized *f*-CNH 3 can be attributed to the two following factors: (i) the strong amplification of the electromagnetic fields near the conical-end of CNHs; note that it is well known that pentagons denote defects within the surrounding aromatic hexagonal network and preferential reactivity to cycloadditions is observed at the conical-tip of CNHs;[18] and (ii) the effect of chemical binding which is mostly related to changes in the electronic structure of the terthiophene unit and their relative orientation relative to the CNH surface.[19] In addition, the UV-spectroscopic characterization of *f*-CNH 3 and the remaining functionalized nanocarbons excluded any resonance Raman effect. *f*-CNH 3 and *f*-CNT 3 displayed a broad absorbance band between ~330 nm to ~530 nm attributed to the terthienyl unit, while the rest of materials displayed no bands related to the thienyl units (Fig. S12, ESI†).

In conclusion, CNHs functionalized with oligothiophene units were synthesized under microwave irradiation and solvent-free conditions. Raman spectra of the *f*-CNH 3 exhibited extraordinary properties barely described for carbon nanostructures. To the best of our knowledge, this is the first example reported in literature where the covalent functionalization of this category of materials induces SERS activity. These findings open a new window for the implementation of CNHs in Raman imaging. *In silico* investigations helped us to rationalize the observed Raman enhancement, which was attributed to the intensification of the electromagnetic fields on the tips of *f*-CNH 3 accompanied by the change of the CNH electronic structure upon functionalization. We consider that the present work will benefit the achievement of a higher understanding of the Raman fingerprint of upcoming functionalized carbon nanostructures and motivate the development of CNHs-based Raman applications.

This work is supported by Iberdrola Foundation (CONV120313), the Spanish Ministerio de Economía y Competitividad (CTQ2017-88158-R), the Junta de Comunidades de Castilla-La Mancha (SBPLY/17/180501/000204) and FEDER-JCCM (UNCM13-1E-1663). The work at the University of Málaga was funded by the MINECO (CTQ2015-66897) and Junta de Andalucía (P09FQM-4708) projects. M. I. L. acknowledges MINECO for her Juan de la Cierva-formación grant (FJCI-2016-29593). The authors acknowledge the computer resources, technical expertise, and assistance provided by the Supercomputing and Bioinformatics centre of the University of Malaga.

Conflicts of interest

There are no conflicts to declare.

Notes and references

1 J. Langer *et al.ACS Nano*, 2020, **14**, 28–117.
2 X. Wang, C. Wang, L. Cheng, S. T. Lee and Z. Liu, *J. Am. Chem. Soc.*, 2012, **134**, 7414–7422.
3 Z. Liu, X. Li, S. M. Tabakman, K. Jiang, S. Fan and H. Dai, *J. Am. Chem. Soc.*, 2008, **130**, 13540–13541.
4 X. Ling, L. Xie, Y. Fang, H. Xu, H. Zhang, J. Kong, M. S. Dresselhaus, J. Zhang and Z. Liu, *Nano Lett.*, 2010, **10**, 553–561.
5 G. McNay, D. Eustace, W. E. Smith, K. Faulds and D. Graham, *Appl. Spectrosc.*, 2011, **65**, 825–837.
6 G. Bodelón, V. Montes-García, V. López-Puente, E. H. Hill, C. Hamon, M. N. Sanz-Ortiz, S. Rodal-Cedeira, C. Costas, S. Celiksoy, I. Pérez-Juste, L. Scarabelli, A. La Porta, J. Pérez-Juste, I. Pastoriza-Santos and L. M. Liz-Marzán, *Nat. Mater.*, 2016, **15**, 1203–1211.
7 S. Feng, M. Cristina dos Santos, B. R. Carvalho, R. Lv, Q. Li, K. Fujisawa, A. L. Elías, Y. Lei, N. Perea-López, M. Endo, M. Pan, M. A. Pimenta and M. Terrones, *Sci. Adv.*, 2016, **2**, 1–13.
8 G. Hong, S. Diao, A. L. Antaris and H. Dai, *Chem. Rev.*, 2015, **115**, 10816–10906.
9 J. Bartelmess, S. J. Quinn and S. Giordani, *Chem. Soc. Rev.*, 2015, **44**, 4672–4698.
10 N. Karousis, I. Suarez-Martinez, C. P. Ewels and N. Tagmatarchis, *Chem. Rev.*, 2016, **116**, 4850–4883.
11 D. Iglesias, J. Guerra, M. V. Gómez, A. M. Rodríguez, P. Prieto, E. Vázquez and M. A. Herrero, *Chem. - A Eur. J.*, 2016, **22**, 11643–11651.
12 V. S. Tiwari, T. Oleg, G. K. Darbha, W. Hardy, J. P. Singh and P. C. Ray, *Chem. Phys. Lett.*, 2007, **446**, 77–82.
13 L. Litti, J. Reguera, F. J. Garciá De Abajo, M. Meneghetti and L. M. Liz-Marzán, *Nanoscale Horizons*, 2020, **5**, 102–108.
14 C. Cioffi, S. Campidelli, F. G. Brunetti, M. Meneghetti and M. Prato, *Chem. Commun.*, 2006, 2129–2131.
15 N. Rubio, M. A. Herrero, M. Meneghetti, Á. Díaz-Ortiz, M. Schiavon, M. Prato and E. Vázquez, *J. Mater. Chem.*, 2009, **19**, 4407–4413.
16 S. Utsumi, H. Honda, Y. Hattori, H. Kanoh, K. Takahashi, H. Sakai, M. Abe, M. Yudasaka, S. Iijima and K. Kaneko, *J. Phys. Chem. C*, 2007, **111**, 5572–5575.
17 I. D. Petsalakis, G. Pagona, N. Tagmatarchis and G. Theodorakopoulos, *Chem. Phys. Lett.*, 2007, **448**, 115–120.
18 S. Park, D. Srivastava and K. Cho, *Nano Lett.*, 2003, **3**, 1273–1277.
19 J. C. Charlier and G. M. Rignanese, *Phys. Rev. Lett.*, 2001, **86**, 5970–5973.